A Single Binding Mode of Activated Enediyne C1027 Generates Two Types of Double-Strand DNA Lesions: Deuterium Isotope-Induced Shuttling between Adjacent Nucleotide Target Sites†

Yong-jie Xu,‡,§ Zhen Xi,‡ Yong-su Zhen,§ and Irving H. Goldberg*,‡

Department of Biological Chemistry and Molecular Pharmacology, Harvard Medical School, Boston, Massachusetts 02115, and Institute of Medicinal Biotechnology, Chinese Academy of Medical Sciences, Tiantan, Beijing 100050, China

Received June 2, 1995; Revised Manuscript Received July 21, 1995⊗

ABSTRACT: It has been previously reported that the potent enediyne antitumor antibiotic C1027 chromophore produces in DNA restriction fragments double-strand lesions at the sequence GTTA1T/ATA2A3C (damage positions are numbered), involving A1 and A3 [Xu, Y.-j., Zhen, Y.-s., & Goldberg, I. H. (1994) *Biochemistry 33*, 5947−5954]. Using oligodeoxynucleotide substrates, an additional double-strand lesion has been found within this sequence to involve A1 and A2. The lesions, which include strand breaks and abasic sites, are due to hydrogen atom abstraction from C4′ at A1 and from C5′ at A3 or C1′ at A2 by the diradical species of activated drug. Lesions at A2 or A3 are always part of double-strand lesions. The drug radical center involved in attack at A2 or A3 is readily quenched by solvent methanol so as to produce a single-strand lesion at A1. By using methanol containing carbon-bound deuterium, there is a substantial isotope effect on the quenching reaction, resulting in enhanced double-strand lesion formation. In the absence of methanol, almost all damage at A1 belongs to double-strand lesions. There is a considerable flexibility of the drug radical attacking A2 or A3, such that the presence of deuterium at C1′ of A2 results in substantial shuttling of the attack to the C5′ of the neighboring nucleotide A3. These data strongly suggest the presence of a single mode of binding of activated drug but one which permits the drug diradical center attacking A2 or A3 to have considerable leeway in target selection. Quantitative affinity cleavage binding analysis is consistent with this proposal.

The new macromolecular antitumor antibiotic C1027, produced by *Streptomyces globisporus* C1027 (Hu et al., 1988), shows extreme potency to cultured cancer cells and marked growth inhibition of transplantable tumors in mice and human cancers inoculated in nude mice (Zhen et al., 1989, 1994). Like other macromolecular antibiotics, such as neocarzinostatin, C1027 is composed of an apoprotein and a labile chromophore. The apoprotein is a single polypeptide chain of 110 amino acid residues cross-linked by two disulfide bonds (Otani et al., 1991). The chromophore, which is noncovalently bound to the apoprotein, is a member of the rapidly enlarging enediyne family of potent antitumor antibiotics (Minami et al., 1993; Iida et al., 1993; Figure 1A) such as neocarzinostatin chromophore (Goldberg & Kappen, 1994), the calicheamicins (Lee et al., 1991; Zein et al., 1988), the esperamicins (Long et al., 1989), the dynemicins (Sugiura et al., 1990), kedarcidin chromophore (Leet et al., 1993; Zein et al., 1993), and the recently found maduropeptin chromophore (Schroeder et al., 1994). The antitumor activity of C1027 is believed to result from intracellular DNA damage by its chromophore (Xu et al., 1990, 1992; McHugh et al., 1995). The noncovalently bound apoprotein stabilizes and controls the release of the labile chromophore for interaction with its cellular DNA target (Okuno et al., 1994).

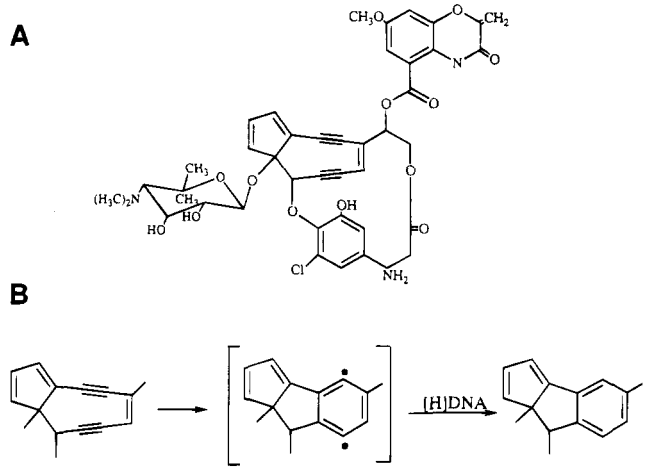

FIGURE 1: (A) Chemical structure of C1027 chromophore and (B) proposed mechanism of activation of C1027 chromophore.

C1027 chromophore consists of two functional domains, i.e., the enediyne core moiety, and the benzoxazonilate and sugar moieties, which are presumably involved in the placement of the enediyne moiety in the minor groove of DNA. The chromophore is proposed to undergo a Bergman-type rearrangement of the enediyne core to form a highly reactive benzenoid diradical species (Figure 1B). The diradical, positioned in the DNA minor groove, abstracts hydrogen atoms from the deoxyribose of the backbone and inititates a series of oxidative DNA damage reactions (Figure 2). Precise positioning of the diradical in the minor groove, which depends on the geometry of the interaction of the drug

† This work was supported by U.S. Public Health Service Grant CA44257 from the National Institutes of Health.

* To whom correspondence should be addressed.
‡ Harvard Medical School.
§ Chinese Academy of Medical Sciences.

⊗ Abstract published in *Advance ACS Abstracts,* September 1, 1995.

0006-2960/95/0434-12451$09.00/0

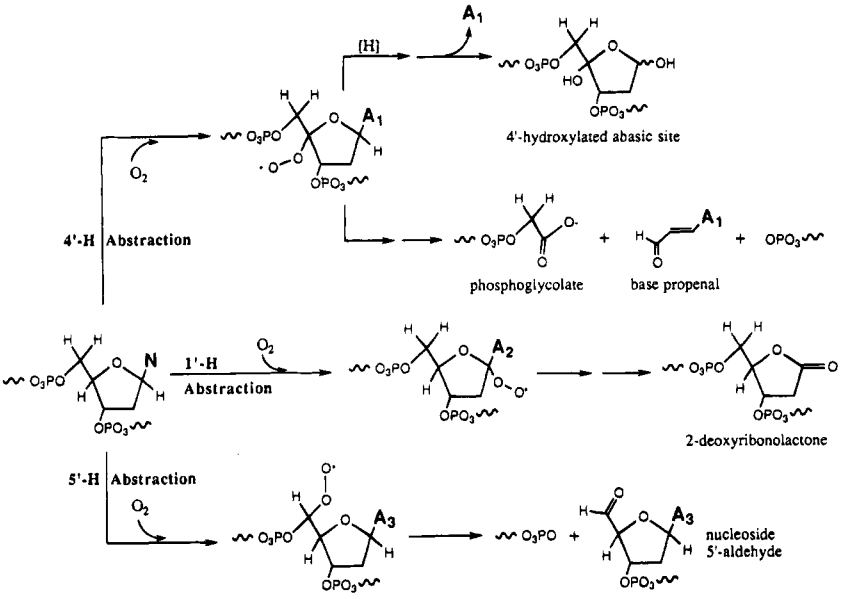

FIGURE 2: Proposed mechanisms for C1027 chromophore-induced DNA damage at A1−A3 sites of the model GTTA1T/ATA2A3C sequence by C4′, C1′, and C5′ hydrogen abstractions, respectively.

molecule and DNA microstructure, has the potential to cause double-strand (DS) damage. Experiments with plasmid and ^{32}P-end-labeled DNA restriction fragments have demonstrated that the single-strand (SS) lesions, which are mainly produced at adenylate and thymidylate residues, are base-specific, while DS lesions show a five-nucleotide sequence specificity, such as at CTTTT/AAAAG, ATAAT/ATTAT, CTTTA/TAAAG, CTCTT/AAGAG, and especially GTTAT/ATAAC (cutting sites are underlined) sequences (Xu et al., 1994), with a two-nucleotide 3′-stagger of the cleaved residues. Cleavage at the site on the positive strand involves C4′ chemistry (Sugiura & Matsumoto, 1993; Xu et al., 1994), whereas that on the negative strand is due to C5′ chemistry (Xu et al., 1994). Since chemical identification and quantitation of the products of the DNA lesions, especially minor lesions, by sequencing long DNA restriction fragments may be analytically difficult, we have turned to the use of oligonucleotides are targets for this drug.

In the present investigation, the damage products at the most preferred target sequence GTTA1T/ATA2A3C (damage positions are numbered) were separately identified and quantitated. While studying cleavage at A1 and A3, an additional strong attack site at A2 was found within the same sequence and shown to be due to C1′ chemistry. By using specifically designed oligomer substrates and observing deuterium isotope effects, it was possible to show that the lesions at A2 or A3 were always part of DS lesions and that a single binding form of the drug diradical was likely responsible for the DS lesiosn at A2 or A3. Further, the extent of involvement of A1 in SS or DS lesions could be shown to depend on the access of solvent methanol to the drug radical center involved in A2 or A3 attack. In the absence of methanol or using deuteriated methanol, almost all of the lesions at the three damage sites were involved in DS lesions and ca. 68% of the decrease in attack at A2 by position-specific deuteriation at C1′ of A2 was unprecedently shifted to A3. These findings have significant implications for the nature of the complex formed between activated drug and its DNA target.

MATERIALS AND METHODS

Materials. Holoantibiotic C1027 was purified from the fermentation broth of the producing *S. globisporus* C1027 strain as reported (Otani et al., 1988). C1027 chromophore was extracted from the apoprotein−chromophore complex with ice-cold methanol containing 0.5 M acetic acid. After centrifugation for 10 min, the supernatant was decanted and evaporated to dryness. The extracted chromophore was dissolved in ice-cold methanol, and insoluble solids were removed by filtering with a 0.22 μm filter. The resulting chromophore solution was stored in the dark at −70 °C (Xu et al., 1994). [γ-^{32}P]ATP, [α-^{32}P]-3′-deoxyadenosine 5′-triphosphate, and [α-^{32}P]cordycepin 5′-triphosphate were purchased from New England Nuclear DuPont. T4 polynucleotide kinase, terminal deoxynucleotidyl transferase, and the Klenow fragment of DNA polymerase I were obtained from New England Biolabs and Promega. Methanol-methyl-d_3 (^{2}H, 99.5%) was purchased from Cambridge Isotope Laboratories. Other chemical reagents were purchased from Sigma and Aldrich.

Synthesis of 5′-(Dimethoxytrityl)-1′-deuteriumyl-2′-deoxy-3′-(cyanoethyl)adenosine Phosphoramidite. The deuterium at C1′-position of ribose was introduced by diisobutylaluminum deuteride reduction of γ-D-ribonolactone; deuteriation was more than 98% as judged by 500 MHz NMR. Ribonucleoside synthesis and 2′-deoxygenation of adenosine was carried out using the procedures of Vorbrüggen (Vorbrüggen & Bennua, 1981) and Robins (Robins et al., 1983), respectively. The phoshoramidite derivative was synthesized by standard methodology.

Oligodeoxyribonucleotide Synthesis. All oligodeoxyribonucleotides were synthesized on an Applied Biosystems 381A automatic synthesizer by the phosphoramidite method. Phosphoramidites and other reagents used for the DNA synthesizer were purchased from Glen Research. The specific nucleotide containing Cl′ deuterium label was incorporated manually into the oligomers using standard phosphoramidite methodology. The triethylene glycol chemical linker [see Yang et al. (1995)] joining the 5′-end of the

FIGURE 3: Sequences of oligodeoxyribonucleotides. Drug interaction sequences, AGT/GCT for neocarzinostatin and GTTA1T/ATA2A3C, are printed in boldface. L1 and L2 are hairpin oligomers with a hexaethylene glycol group, X, which holds the positive and the negative strands together via two phosphodiesters.

positive strand and the 3′-end of the complementary strand via two phosphodiester bonds (L1 and L2, Figure 3) was also incorporated manually. The concentrations of single-strand oligomers were determined by UV absorbance at 260 nm. Oligomers were 5′-end-labeled with ^{32}P by T4 polynucleotide kinase, and the 3′-end of oligomers were ^{32}P-end-labeled by either the Klenow fragment of DNA polymerase I or terminal deoxynucleotidyl transferase. The labeled oligomers were purified by electrophoresis on 20% polyacrylamide gels containing 8.3 M urea.

DNA/Drug Reaction. The 5′- and 3′-end-labeled oligomers were annealed to their complementary strands (1:1.5 ratio) by heating at 90 °C for 3 min and slow cooling to room temperature (Kappen & Goldberg, 1992a,b). A standard reaction mixture contained 20 mM Tris·HCl (pH 8.0), 1 mM EDTA, and 10 μM (phosphate) ^{32}P-end-labeled oligomers. Before adding drug, the mixture was precooled in ice for 5−10 min. To initiate the DNA/drug reaction, the drug was added to 10 μM in the methanol vehicle, and a control received an equal volume of methanol (10%, v/v). To remove the methanol in the reaction, the reaction mixture was quickly frozen, evaporated to dryness, and then dissolved in a equal amount of H_2O. The reaction was allowed to proceed in the dark at 0 °C for 6 h or overnight and stopped by drying in a Speed-Vac concentrator. When holo-C1027 was used, the reaction was carried out in 10 mM phosphate buffer (pH 8.0) at room temperature. Alkaline treatment involved heating one of the duplicate aliquots in 50 μL of 1 M piperidine at 90 °C for 30 min. The piperidine was then removed by drying three times in H_2O. As for hydrazine treatment, hydrazine hydrochloride (pH 8.0) was added to a final concentration of 100 mM and incubated for 1 h at room temperature.

Analysis of DNA Damage Products by Gel Electrophoresis. The final dried sample pellets were redissolved in 80% (v/v) formamide, containing 1 mM EDTA and marker dyes, and electrophoresed on a 20% sequencing polyacrylamide gel (National Diagnostics). The gel band intensities were quantitated by scanning with a Molecular Dynamics PhosphorImager instruments, and the data were analyzed by performing volume integration using Image Quant software version 3.22. The bands of interest were sometimes excised from the gel and crushed, and the oligomers were eluted by stirring overnight at 4 °C in Tris buffer (pH 8.0). Samples were dried and then dissolved in H_2O for further analysis.

Quantitative Affinity Cleavage Titration. The 3′-end-labeled L1 oligomer (Figure 3) was annealed and precooled as described above. The quantitative affinity cleavage experiment was performed in 20 mM Tris buffer containing 1 mM EDTA and 30 000 cpm of oligomer (pH 8.0) in the presence of methanol (10%). The C1027 chromophore was added in various concentrations to initiate the drug reaction. The reaction mixture was incubated in ice overnight and stopped by drying. The dried pellet was then treated with 1.0 M piperidine to cleave all alkali-labile abasic sites. The cleavage products of the oligomer were separated by a sequencing gel and quantitated. The binding curve for each specific cleavage site, represented by the following equation, where I_{site} is the intensity of the band at each cleavage site, I_{max} is the apparent maximum cleavage, [drug] is the C1027 concentration, and K_b is the equilibrium association constant for C1027 chromophore, was fitted to the experimental data using I_{max} and K_b as adjustable parameters:

$$I_{site} = I_{max} \frac{K_b[\text{drug}]}{1 + K_b[\text{drug}]} \quad (1)$$

The difference between I_{fit} and I_{site} for all data points was minimized using the fitting procedure of KaleidaGraph software running on a Macintosh computer (Han & Dervan, 1993; Stassinopoulos & Goldberg, 1995).

Determination of Site-Specific Isotope Effects. The drug/DNA oligomer reactions were performed identically and in parallel for a given pair of [^1H]- and [^2H]oligonucleotides. The DNA damage products were separated and the cleavage efficiencies at the specific position analyzed using the Molecular Dynamics PhosphorImager instrument as described above. An identical site, but having only protium, in the same oligonucleotide acted as an internal control.

Quantitation of Strand Breaks in pBR322 Plasmid. pBR322 DNA (25 μg/mL) was treated with different concentrations of holo-C1027 or its chromophore (10% methanol) in 20 mM Tris·HCl buffer, pH 8.0. The reaction was carried out overnight in ice in the dark. To reveal the abasic lesions, the DNA was further treated with 100 mM putrescine for 1 h at 37 °C. The changes in topological forms were analyzed by agarose gel electrophoresis and quantitated by a laser densitometer. The number of DS and SS breaks in pBR322 was calculated from the relative quantities of the three plasmid forms by assuming a Poisson distribution of the cleavage sites (Xu et al., 1994).

RESULTS

Analysis of Lesion Due to C4′ Chemistry at A1 of GTTA1T/ATA2A3C. Our previous study using a 307 bp 5′-^{32}P-labeled restriction fragment demonstrated that at the GTTA1T/ATA2A3C sequence, C1027 caused DS lesions involving A1 and A2. A band corresponding to cleavage at A1 of GTTA1T migrated slightly faster than the 3′-phosphate-ended marker. The electrophoretic mobility of the band suggested the formation of a fragment with a 3′-phosphoglycolate end, such as is produced by abstraction of the C4′ hydrogen (Xu et al., 1994). To characterize the C4′ chemistry at this site in greater detail, we synthesized a DNA oligomer, 5′CGTTA1TGTTA1TGC (Figure 3, D1), containing two cleavage

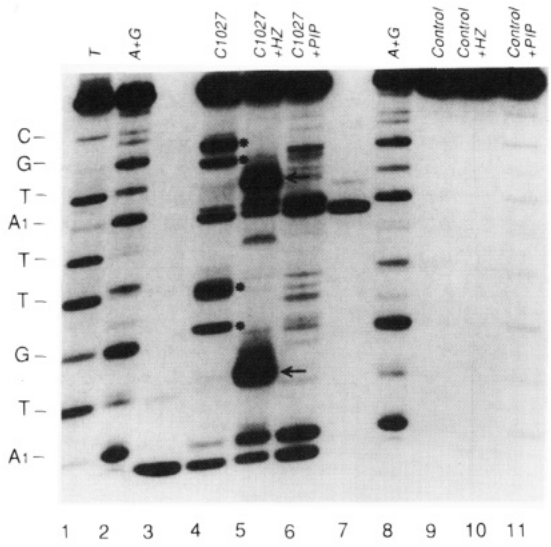

FIGURE 4: C1027 chromophore-induced damage at the A1 site of the GTTA1T/ATA2A3C sequence. 5′-^{32}P-End-labeled d(CGTTA1TGTTA1TC) was annealed with its complementary d(GATA2A3CATA2A3CG) strand and incubated with C1027 chromophore under the conditions described in Materials and Methods (lanes 4−6). Control reactions received the same amount of methanol (10%) (lanes 9−11). Lane 1, 2, and 8 are T and A + G Maxam−Gilbert markers; lanes 3 and 7 are synthesized 5′-^{32}P-end-labeled d(CGTT) and d(CGTTATGTT) markers having 3′-phosphoglycolate termini, respectively; lanes 5 and 10, and 6 and 11 are samples treated with hydrazine (HZ) and piperidine (PIP), respectively. The bands indicated by arrows represent the 3′-phosphopyridazine derivative, and the slow moving bands shown by asterisks are explained in the text.

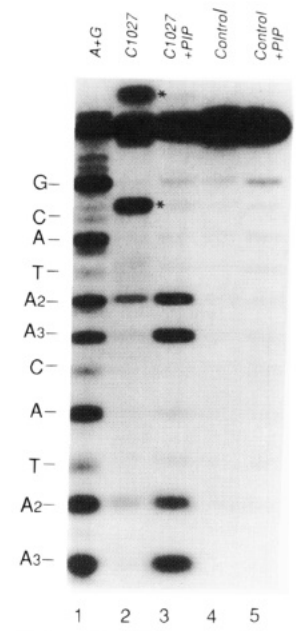

FIGURE 5: Gel analysis of the damage at A2 and A3 of GTTA1T/ATA2A3C. 3′-^{32}P-End-labeled d(GATA2A3CATA2A3CG) duplexed with d(CGTTA1TGTTA1TC) was treated with C1027 chromophore (lanes 2 and 3) or methanol control (lanes 4 and 5) and then with piperidine (lanes 3 and 5) as described in Materials and Methods. A + G are Maxam−Gilbert markers. Asterisks indicate the markedly slow moving bands of oligo fragments terminated with nucleoside 5′-aldehyde.

sites (numbered) and its complementary 5′GCATA2A3CATA2A3CG (Figure 3, D2) strand. The reason for including two cleavage sites is to enable change in the sequence or chemical modification of one of the two sites while leaving the other as an internal control. The results of analysis by high-resolution gel electrophoresis of the reaction of C1027 chromophore with the 5′-^{32}P-D1 duplexed with its complementary strand D2 are shown in Figure 4. DNA cleavage by C1027 chromophore afforded exclusively two fragments at each site which run slightly faster than the Maxam−Gilbert 3′-phosphate-ended markers, but comigrate with authentic oligomers having 3′-phosphoglycolate termini (compare lanes 3 and 4, 6 and 7 at A1 sites). The slow moving bands, designated by asterisks (lane 4), likely represent degradation products of the 4′-hydroxylated abasic lesion at the A1 site (Kappen & Goldberg, 1992a). Treatment with hydrazine generated slower moving bands that are consistent with the electrophoretic behavior of the 3′-phosphopyridazine derivative (Kappen et al., 1991) due to adduct formation with the 4′-hydroxylated product (Figure 2). The increase of the fragments with 3′-phosphate ends in lane 5 at A1 was probably caused by breakage of abasic sites during the workup with hydrazine. Alkali-labile abasic sites were expressed by treatment with piperidine, resulting in a marked increase of the band intensities of the fragments with 3′-phosphate ends (Figure 4, lane 6). The DNA damage products analyzed at A1 of GTTA1T/ATAAC were identical with those due to C4′ chemistry (Figure 2) induced by bleomycin (Giloni et al., 1981; Stubbe & Kozarich, 1987) and neocarzinostatin (Kappen et al., 1991). Quantitation of the slower 3′-phosphopyridazine and the faster 3′-phosphoglycolate bands showed that at least 96% of the lesion at the A1 of the GTTA1T sequence is due to C4′ hydrogen abstraction.

Analysis of Lesion Due to C5′ Chemistry at A3 of GTTA1T/ATA2A3C. C1027 chromophore treatment of the 3′-end-labeled oligomer 5′GCATA2A3CATA2A3CG (Figure 3, D2) containing two ATA2A3C sequences, duplexed with its complementary strand D1, generated two slow bands (Figure 5, lane 2, indicated by asterisks). After alkaline treatment, the slow bands disappeared and the intensities of the bands at the A3 sites were accordingly enhanced (lane 3). In a separate experiment, the two slow bands were isolated from the gel, treated with piperidine, and reloaded on a gel, and the products comigrated with A3 of the 5′-phosphate bands of each of the two target sequences (data not shown). The electrophoretic behavior of the slow bands strongly suggested that they were fragments terminated with 5′-aldehyde, the diagnostic product of C5′ chemistry, such as is produced by neocarzinostatin at the T of ACT/AGT (Figure 2; Kappen & Goldberg, 1983; Kappen et al., 1991). Alkaline treatment resulted in elimination of the 5′-aldehyde moiety to afford a 5′-phosphate-ended fragment. Quantitation of the 5′-phosphate and 5′-aldehyde bands showed that more than 95% of the lesion at the A3 site of GTTA1T/ATA2A3C was induced by C5′ hydrogen abstraction.

Analysis of Lesion Due to C1′ Chemistry at A2 of GTTA1T/ATA2A3C. As shown in Figure 5, cleavage was markedly enhanced at A2 after alkali treatment, suggesting that an abasic lesion had been generated at this site. In order to understand the mechanism of formation of the abasic lesion, two approaches using oligomers have been taken. The first was to compare this lesion with that of AGC/GCT by neocarzinostatin, a well-studied C1′ lesion (Kappen et al., 1988; Kappen & Goldberg, 1989); the other was to observe the position-specific isotope effect utilizing oligomer

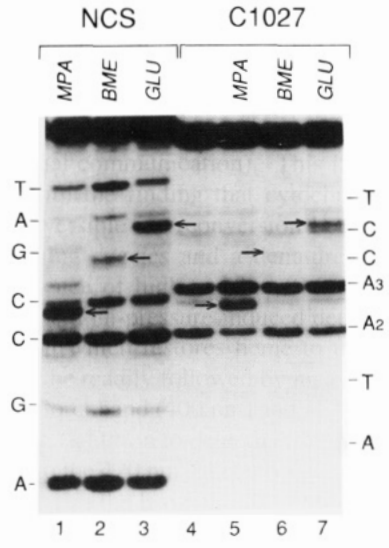

FIGURE 6: Comparison of the thiol-adducted C1′-lesion product at C of AGC by neocarzinostatin and the lesion at A2 of ATA2A3C by C1027. 5′-^{32}P-End-labeled d(TGCAGCCGAT) annealed with d(ATCGGCTGCA) (lanes 1−3) and 5′-^{32}P-end-labeled d(GGCATA2A3CCT) duplexed with d(AGGTTATGCC) (lanes 4−7) were treated with neocarzinostatin or C1027 chromophore in the presence of thiol under the standard conditions (Kappen & Goldberg, 1989), respectively. MPA, 3-mercaptopropionate (3 mM); BME, 2-mercaptoethanol (10 mM); GLU, glutathione (3 mM). Lane 5 is a no-thiol control. The slow moving bands of thiol adducts are indicated by arrows.

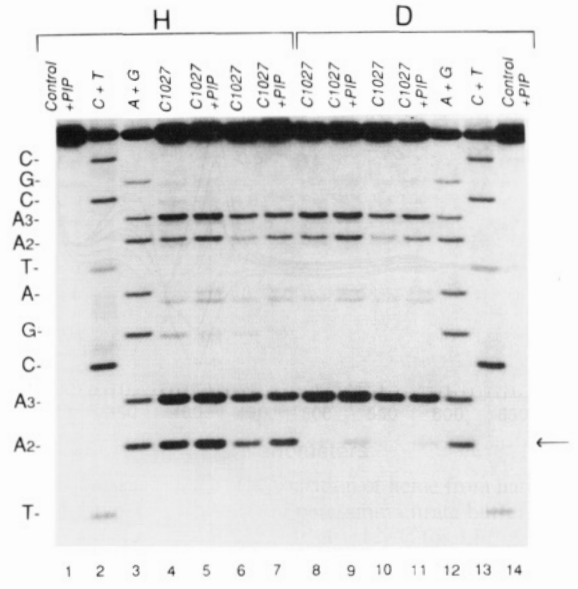

FIGURE 7: Deuterium isotope effect on DNA damage by C1027 chromophore at the A2 site of the ATA2A3C sequence. 5′-^{32}P-End-labeled d(GCATA2A3CGATA2A3CGC) annealed to oligomer d(GCGTTA1TCGTTA1TGC) was treated with 10 μM (lanes 4 and 5, 8 and 9) or 5 μM (lanes 6 and 7, 11 and 12) C1027 chromophore. Lanes 1−7, both A2 sites have C1′-^{1}H; lanes 8−14, one A2 site (indicated by arrow) has C1′-^{2}H. C + T and A + G are Maxam−Gilbert markers. Lanes 5, 7, 9, and 11 are samples treated with piperidine.

5′GCATA2A3CGATA2A3CGC containing a [1′-^{2}H]dA (underlined).

Abstraction of the hydrogen atom from the C1′-position of the C in AGC/GCT by neocarzinostatin chromophore in the presence of dioxygen generates an alkali-labile abasic site consisting of a 2-deoxyribonolactone moiety with intact phosphodiester linkage (Figure 2; Kappen & Goldberg, 1989). In the presence of thiol, there is the formation of thiol adducts of the 3′-unsaturated sugar generated by β-elimination at the 3′-side of the abasic lesion produced by C1′ chemistry (Kappen & Goldberg, 1992a). An experiment using oligomers D3 and D4 (Figure 3) showed that the mobilities of this thiol-adducted C1′-lesion derivative in the neocarzinostatin reaction vary with the chemical structures of the thiols (Figure 6, lanes 1−3). The band associated with the anionic 3-mercaptopropionate adduct moves fastest (lane 1), while the glutathione adduct has the slowest mobility (lane 3), probably due to its bulky structure, as compared with the neutral 2-mercaptoethanol derivative (lane 2).

Experiments with the duplex containing 5′-end-labeled oligomer D6 (Figure 3) revealed that there was no fast 3′-phosphoglycolate band associated with the A2 site (Figure 6, lane 4), which indicates that it was unlikely that the abasic lesion at this site was caused by C4′ hydrogen abstraction. However, when the experiment was done in the presence of different thiols, using the same reaction conditions as for neocarzinostatin, C1027 chromophore induced the formation of slow bands with different mobilities which are consistent with the formation of thiol adducts of lesions due to C1′ chemistry (Figure 6, compare lanes 1−3 with lanes 5−7). In the absence of thiol (Figure 6, lane 4), the band corresponding to a 3′-phosphate band at A2 was probably due to the spontaneous cleavage of the labile abasic lesion. Because the thiol adducts derived from the 4′-hydroxylated abasic site due to C4′ chemistry have different electrophoretic behaviors from those due to the C1′ lesion (Kappen & Goldberg, 1992a,b), the results suggest that the abasic site generated by C1027 chromophore at the A2 of GTTA1T/ATA2A3C is generated by C1′ hydrogen abstraction.

Conclusive proof for C1′ chemistry at the A2 site of GTTA1T/ATA2A3C comes from studies involving specific isotope selection effects (Figure 7), as had been found earlier for neocarzinostatin (Kappen et al., 1990). [1′-^{2}H]dA was specifically incorporated into one of the two attack sites in the D8 oligomer d(GCATA2A3CGATA2A3CGC) (underlined). Incubation of the 5′-end-labeled oligomer, annealed with its complementary strand D7, with C1027 chromophore generated an alkali-dependent cleavage at the two A2 sites (compare lanes 4, 5, and 6, 7). Identical experiments were performed on the same oligomer in which deuterium replaced protium at the C1′ position of A2 at one of the two target sequences (indicated by an arrow). Comparison of lane 5 with 9 and lane 7 with 11 showed a substantial isotope selection effect on C1027-mediated DNA damage at the A2 of GTTA1T/ATA2A3C. Quantitation of the isotope effect by the PhosphorImager instrument gave a remarkable isotope discrimination ($k_H/k_D = 7.05$), which is close to the theoretical maximum, as was also observed with bleomycin at some specific cleavage sites (Worth et al., 1993). Cleavage at the other A2 at the 3′-end of the same oligonucleotide, which contained protium at C1′, was unaffected (compare lanes 5 with 9 and 7 with 11). These results provided strong evidence that the band at A2, both before and after piperidine treatment, results from hydrogen abstraction from C1′ by C1027 chromophore. The lability of the precursor giving rise to this band is also consistent with the oxidative formation of a deoxyribonolactone intermediate (Kappen & Goldberg, 1989).

Virtually All Damage at A2 and A3 Involved DS Lesions. The results described above showed that in DNA duplexes

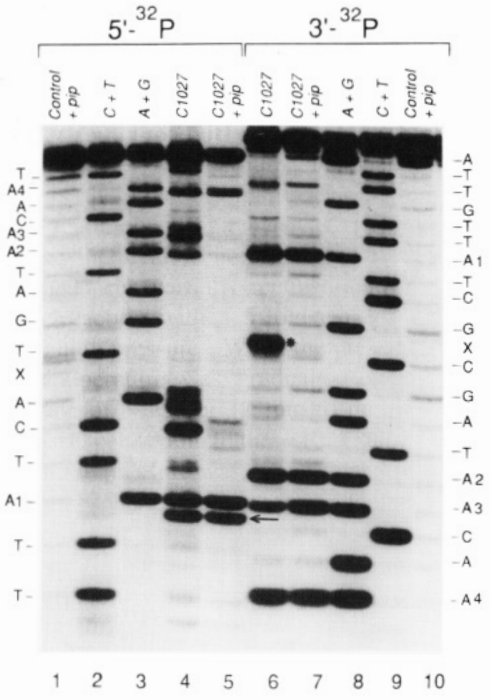

FIGURE 8: Gel analysis of SS and DS lesions within the GTTA1T/ATA2A3C sequence. Hairpin oligomer L1 was 5′- (lanes 1−5) or 3′- (lanes 6−10) ^{32}P-end-labeled and treated with C1027 chromophore as described in Materials and Methods. Samples were dried and aliquots were further treated with piperidine (pip). C + T and A + G are Maxam−Gilbert standard markers. X represents the migration position of the fragment having the chemical linker at its 3′- or 5′-end. The arrow and asterick indicate DNA fragments ended with 3′-phosphoglycolate and nucleoside 5′-aldehyde, respectively.

containing the GTTA1T/ATA2A3C sequence, C1027 can abstract hydrogens from C4′ of A1 and C1′ of A2 or C5′ of A3 resulting in DNA cleavage and abasic lesions. In order to study the relationship of the three damage sites, oligomers ATTGTTA1TCA and TGATA2A3CAA4T containing the model GTTA1T/ATA2A3C sequence and a SS cleavage site, A4, were joined together as a single molecule by a chemical linker (Figure 3, L1). Nondenaturing gel analyses showed that after reannealing, more than 95% of the molecules had a stable hairpin structure (Durand et al., 1990). The hairpins were designed so that drug-induced SS and DS cleavage will generate ^{32}P fragments differing in size, which can be separated by denaturing gels. By labeling with ^{32}P at either the 3′- or 5′-end of the hairpin structure, it is possible to determine which breaks are SS or DS, since in DS lesions only the break closest to the label shows as a band on the gel. Abasic sites that are part of a DS lesion caused the DNA fragment formed by a break to migrate slightly faster, but because the phosphodiester linkage at the abasic site is intact, the fragment acts as though it has only a single lesion. Since the abasic site is closer to the ^{32}P-end label than the other lesion, after alkaline treatment the alkali-induced break will be the only cleavage site seen on the gel.

The cleavage results using 5′- and 3′-^{32}P-end-labeled L1 are shown in Figure 8. Incubation of 5′-end-labeled L1 (lanes 1−5) with C1027 chromophore (10% methanol resulted in four major ^{32}P fragments corresponding to A1−A4 sites, as expected (lane 4). The slow moving bands between X and A1 markers were likely degradation products of the abasic lesion at the A1 site, as shown in Figure 4. Consistent with the results using duplex DNA, the slightly fast moving glycolate bands at the A1 (arrow) and A4 sites indicated that the damage at the two sites was due to C4′ hydrogen abstraction. However, the slightly faster mobilities of the ^{32}P fragments corresponding to A2 and A3 suggested that they had an abasic site between these sites and the 5′-end-label. Since the piperidine treatment, which cleaves the 4′-hydroxylated lesions at the A1 site, caused them to virtually disappear (lane 5), it is clear that the damage at A2 and A3 belong to DS lesions. In contrast to the A2 and A3 bands, the A4 band was resistant to piperidine treatment, as expected, because it resulted from SS cleavage and lacked an abasic site within the sequence. The strong phosphate band at A1 (5′-end-label) and the lack of effect of piperidine on the band at A2 (3′-end-label, see immediately below) are due to breakdown of the abasic sites under these particular workup and gel conditions.

Similarly, experiments using 3′-^{32}P-end-labeled L1 under the same conditions resulted in four major bands relative to the A1−A4 sites (Figure 8, lanes 6−10). The nucleoside aldehyde band in lane 6 (asterisk) was diagnostic of cleavage by C5′ chemistry at the A3 site, consistent with the cleavage pattern found in duplex DNA. The resistance of the band at A1 to alkali showed that it was the product of SS cleavage. Quantitation of this band showed that under the reaction conditions (10% methanol), ca. 40% of the damage of the A1 site was due to SS lesions.

Evidence That the Three Damage Sites at A1−A3 Were Likely Caused by a Single Mode of Drug Binding. The finding that two sets of DS lesions (A1 and A2, A1 and A3) occur within a single target GTTA1T/ATA2A3C sequence is rather unexpected and raises the question as to whether they are due to a single drug-binding mode or result from two different binding modes. To address this question, the binding constant of the drug at each cleavage site was examined by the use of quantitative affinity cleavage titration (Han & Dervan, 1993; Stassinopoulos & Goldberg, 1995). If the three damage sites were caused by more than one drug-binding mode, the drug might bind to the different DNA microstructures with different binding constants. However, the data in Figures 9 and 10 indicated that the binding constants for the A1−A3 cleavage sites were virtually the same ($K_b = 5.98 \pm 0.5\ \mu M^{-1}$) (and binding was of a single type) compared with that for A4 ($K_b = 0.37\ \mu M^{-1}$), a known SS cleavage site (Figure 8). The virtual identity of the binding constants for the cleavage at A1−A3 is necessary but not sufficient for proving the existence of a common binding site. Eventually, the SS cleavage at A4 should be equivalent to the total cleavage at A1−A3 in this system. However, because of multiple-hit kinetics, the intensity of the band at A4 became stronger than that of the total cleavage at A1−A3 as the concentration of the drug reached very high levels (Figure 9). Similar binding constants were obtained in experiments using the hairpin substrate lacking the A4 target site (Figure 3, L2), ruling out the possible influence of secondary cleavage sites. It should also be noted that in contrast with the changing relation between A4 and A2/A3, the ratio of the cleavage at A2 and A3 stays relatively constant over a wide range of drug concentrations, consistent with a single binding mode. These results suggested that the three damage sites of A1−A3 of the GTTA1T/ATA2A3C sequence might be caused by a single binding mode of the C1027 chromophore molecule, i.e., one of the drug diradical centers was responsible for the damage at A1, while the other

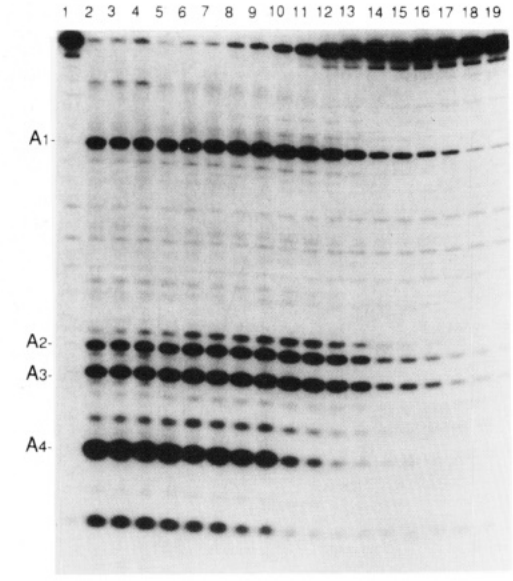

FIGURE 9: Autoradiography of quantitative affinity cleavage titration experiment. Hairpin oligomer L1 was 3′-^{32}P-end-labeled and treated with different concentrations of C1027 chromophore in the presence of methanol (10%). All samples were further treated with piperidine to reveal the abasic sites. The concentrations of drug are 0 μM (lane 1), 50 μM (lane 3), 37.5 μM (lane 3), 25 μM (lane 4), 12.5 μM (lane 5), 5.0 μM (lane 6), 3.75 μM (lane 7), 2.5 μM (lane 8), 1.25 μM (lane 9), 0.5 μM (lane 10), 0.375 μM (lane 11), 0.25 μM (lane 12), 0.125 μM (lane 13), 0.05 μM (lane 14), 0.0375 μM (lane 15), 0.025 μM (lane 16), 0.0125 μM (lane 17), 0.005 μM (lane 18), and 0.00375 μM (lane 19).

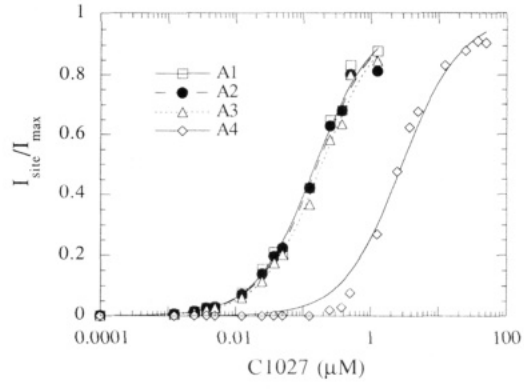

FIGURE 10: Data points quantitated from the autoradiography of Figure 9 normalized to a maximum value of 1 ($I_{max} = 1$) and fitted using eq 1. Curves are the best fit binding titration isotherms for the four damage sites at A1−A4.

could abstract the hydrogens from either the C1′-position of A2 or the C5′-position of A3. Whether cleavage at A1 was a SS lesion or part of a DS lesion involving A2 or A3 was determined by the ability of the other radical center to be quenched by solvent methanol (vide infra).

Effects of Methanol on DS Lesion Formation. Previous work has shown that incubation of pBR322 plasmid DNA with C1027 chromophore generated SS and DS cleavage and that the ratio of DS to SS breaks was 1:4.2 (Xu et al., 1994). After treatment with putrescine, which cleaves virtually all abasic lesions to produce strand breaks, the ratio was changed to ca. 1:1. However, Cobuzzi and colleagues have recently observed a relatively higher frequency of DS cleavage using holo-C1027 (Cobuzzi et al., 1995). It seemed possible that the difference might be due to the presence of methanol (10%) (which was added as a solvent for the C1027 chromophore) in the chromophore reaction. As shown in

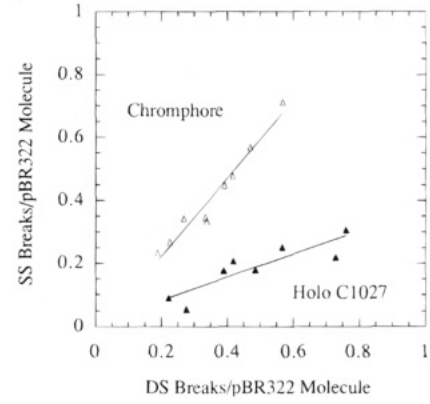

FIGURE 11: Quantitation of DS and SS breaks produced by C1027 chromophore or holo-C1027 in pBR322 DNA. pBR322 DNA was incubated with different concentrations of C1027 chromophore (10% methanol) or holo-antibiotic. Samples were then treated with putrescine to break the abasic lesions. The changes in topological forms of the plasmid were analyzed by agarose gel electrophoresis. The number of DS and SS breaks was calculated from the relative quantities of the three topological forms: (△) C1027 chromophore and (▲) holo-C1027.

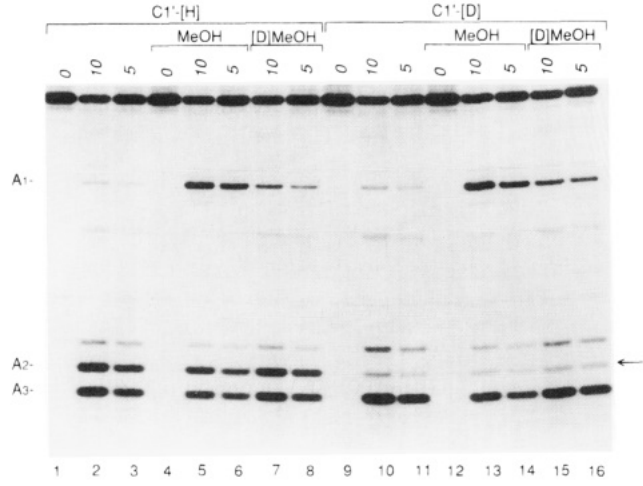

FIGURE 12: Deuterium-induced shuttling of nucleotide attack site and the effects of methanol on DS lesion formation. 3′-^{32}P-End-labeled hairpin oligomer L2 containing either ^{1}H (lanes 1−8) or ^{2}H (lanes 9−16) at the C1′-position of A2 was treated with 5 or 10 μM holo-C1027 in the absence (lanes 1−3 and 9−11) and presence (lanes 4−6 and 12−14) of methanol or methanol-methyl-d_3 (lanes 7, 8, 15, and 16). All samples were treated with piperidine to express alkali-labile lesions. The three damage sites at A1−A3 are marked on the left. The arrow on the right indicates the A2 nucleotide which was substituted with deuterium at the C1′-position.

Figure 11, after putrescence treatment the ratio of DS to SS breaks generated by C1027 chromophore in the presence of methanol was 1:1.2, consistent with our previous observation. When the plasmid DNA was incubated with holo-C1027 in the absence of methanol, however, the ratio was increased to 1.8:1.

To further elucidate the mechanism whereby methanol interferes with DS lesion formation, 3′-^{32}P-end-labeled hairpin oligomer L2 (Figure 3), containing only one GTTA1T/ATA2A3C interaction sequence, was used as the substrate for the cleavage reaction. As shown in Figure 12, lanes 2 and 3, in contrast with the results in Figure 8 with C1027 chromophore, the damage at A1 was almost exclusively involved in DS lesions when L2 was incubated with holo-C1027 (Table 1). However, when the cleavage was done in the presence of 10% methanol, a significant part of the

Table 1: Effects of Methanol on DS Damage Formation and Deuterium-Induced Shuttling of Nucleotide Attack Site[a]

	oligo L2											
	C1′-[H]A2						C1′-[^{2}H]A2					
	−MeOH		+MeOH		+[^{2}H]MeOH		−MeOH		+MeOH		+[^{2}H]MeOH	
C1027 (μM)	10	5	10	5	10	5	10	5	10	5	10	5
cleavage at A1[b]	2.1	1.2	21.0	13.3	6.4	4.1	3.5	2.0	27.0	15.8	9.8	6.2
A2	22.6	13.7	13.4	7.9	19.8	12.0	4.6	2.8	2.9	1.7	3.8	2.3
A3	26.9	15.5	15.1	9.2	22.4	13.6	39.1	22.8	18.8	10.5	30.2	17.4
T[c]	4.5	3.3	2.3	1.5	3.7	2.3	6.9	4.1	3.0	1.8	5.1	3.4
total cleavage	56.1	33.7	51.8	31.9	52.3	32.0	54.1	31.7	51.7	29.8	48.9	29.3

[a] Results of the quantitation of data from Figure 12 by the PhosphorImager instrument. [b] Cleavage efficiencies are expressed as percentages of total DNA. [c] T is the neighboring nucleotide at the 5′-side of A2.

damage at A1 was changed to SS lesions (Figure 12, compare lanes 2 and 3 with 5 and 6), consistent with the results of Figure 8. The amount of SS lesions at A1 was found to be dependent on the concentration of methanol in the drug/DNA reaction (data not shown). Because the damage at A2 and A3 was always a component of DS lesions (Figure 8), it seems that only the radical center which attacks either A2 or A3 can be affected by methanol. Total cleavage (SS plus DS) was little affected by the methanol (Table 1).

The question arises as to whether the methanol interfered with attack at A2 or A3 because of changes in the physical structure of the complex or because it was an effective and selective quencher of one of the radical centers on the drug in the complex. To address this issue, experiments (Figure 12) were conducted in which the methanol either contained protium entirely (lanes 4−6) or deuterium lanes 7−8) in the methyl moiety. As shown in Figure 12, in experiments using CD_3OH, the bands corresponding to SS cleavage at A1 (lanes 7 and 8) were markedly decreased ($k_H/k_D = 3.3$), so that ca. 90% of the damage at A1 belongs to DS damage; the DS lesions at A2 and A3 correspondingly increased, with the total cleavage being unchanged (Table 1) compared with reactions using CH_3OH (lanes 5 and 6). In a separate experiment, in which the methanol was removed from the reaction mixture by quickly freezing and drying after the chromophore was added, the results were found to be similar to that shown in Figure 12 and Table 1 for holo-C1027 (data not shown). The results suggested that solvent methanol strongly quenched one of the drug diradical centers, the one which was flexibly positioned between the C1′ of A2 and the C5′ of A3, resulting in fewer DS lesions.

Deuterium-Induced Shuttling of Attack between Adjacent Nucleotides. The model of DNA damage shown in Figures 2 and 13 proposes that when C1027 chromophore binds to the GTTA1T/ATA2A3C sequence, it directly generates a diradical species; one of the radicals attacks the C4′-position of A1 and the other abstracts a hydrogen atom from either C1′ of A2 or C5′ of A3. In the experiment with C1027 chromophore in which deuterium was substituted for the C1′ hydrogen of A2 (Figure 7), the substantial decrease in attack at A2 was associated with only a slight increase (ca. 10% of the lesion at A2) in the attack at A3. Because this experiment was done in the presence of methanol (10%), it was possible that shuttling of the attack site to a different carbon site on the same nucleotide, such as described for neocarzinostatin (Kappen et al., 1991), or to the adjacent nucleotide A3 was interfered with by solvent quenching. Also, since these experiments involved electrophoretically separated strands of duplex DNA, it was not possible to determine the extent to which DS and SS lesions were affected.

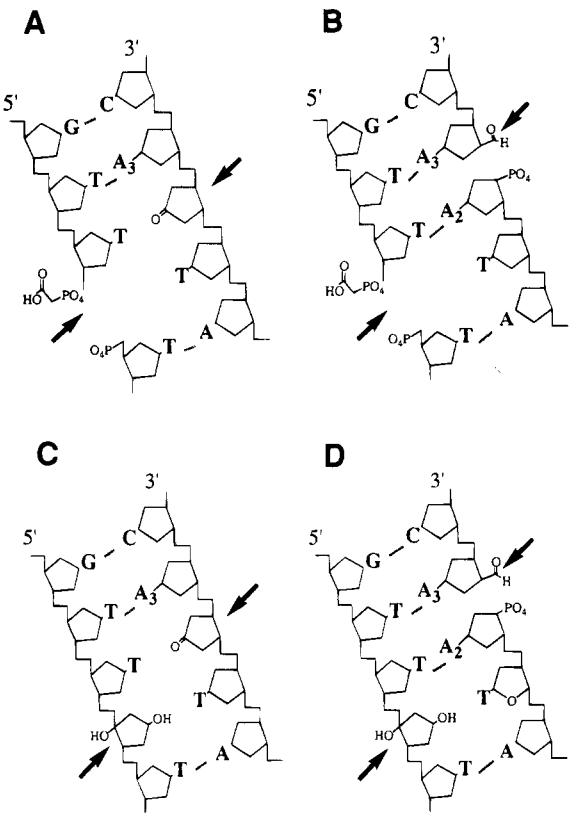

FIGURE 13: Stylized models of C1027-induced DS lesions in the GTTA1T/ATA2A3C interaction sequence. A and C are the one-nucleotide 3′-staggered DS lesions involving A1 and A2; B and D are the two-nucleotide 3′-staggered DS lesions involving A1 and A3.

To determine possible deuterium isotope effects on the DS lesion induced by C1027, we prepared the L2 hairpin oligomer (Figure 3) in which the A2 nucleotide had ^{2}H at the C1′-position (Figure 12, lanes 9−16, indicated by an arrow). The specifically ^{2}H-labeled L2 was 3′-^{32}P-end-labeled and treated with holo-C1027 in the absence of methanol. The cleavage products were analyzed and quantitated under identical reaction conditions (Figure 12, lanes 9−16; Table 1). It was found that ca. 68% of the loss of damage at A2 due to the isotope effect was shifted to A3 by the position-specific deuterium substitution (compare lanes 2 and 3 with 10 and 11). There was little change in SS lesion formation at A1. In two additional sets of similar experiments, involving several levels of drug, the extent of transfer varied from 50% to 60% (data not shown). Consistent with the data in Figure 7, only a slight amount of the attack of A2 was shifted to A3 in the presence of 10% methanol (compare lanes 5 and 6 with 13 and 14; Table 1).

However, in the presence of deuteriated methanol, the extent of the shift was increased to about the level found in the absence of methanol (compare lanes 7 and 8 with 15 and 16; Table 1).

DISCUSSION

C1027 chromophore, like other enediyne antitumor antibiotics, can generate DS lesions in duplex DNA in a sequence-dependent manner. The ability of these agents to form DS lesions derives from the fact that the active form of the drug is a diradical species, each radical center of which has the capability to abstract hydrogens from deoxyribose carbons of the complementary DNA strands that are accessible from the minor groove. The success rate of the bifunctional drug in creating DS lesions appears to vary from drug to drug (Dedon & Goldberg, 1992; Dedon et al., 1993) and is strongly dependent on the local microstructure of the DNA at the target site, as well as the precise reaction conditions, since unfruitful quenching of one of the radical centers results in SS lesions. In the case of neocarzinostatin chromophore, one radical center (at C6 of the diradical) is highly efficient in hydrogen abstraction from the T residue in AGT/ACT or AGC/GCT, whereas the other radical center (at C2) is somewhat less successful in hydrogen abstraction from the T or C residue, respectively, on the complementary strand. This results in a substantial number of SS lesions, in addition to DS lesions. As evidence of the more exposed nature of the radical center at C2 of neocarzinostatin is the observation that this radical in the activated drug−DNA complex is readily quenched by solvent methanol, whereas that at C6 is not (Meschwitz et al., 1992; Chin & Goldberg, 1993). Similarly, one of the radical centers of activated C1027 chromophore appears to be highly efficient in abstracting hydrogen from C4′ of A1 in the preferred target sequence GTTA1T/ATA2A3C (D1, Figure 3) and somewhat less so in abstracting hydrogen from C5′ of A3 or C1′ of A2 of the complementary strand (D2, Figure 3). Thus, while lesions at A3 or A2 are always part of DS lesions, SS lesions are also found at A1. The extent of lesion formation on the D2 strand is strongly influenced by DNA microstructure (determined by sequence), as shown by the relatively pure SS lesion at A4 in L1 (Figure 8) and at other target sites (Xu et al., 1994). It is also of interest that in the case of neocarzinostatin the DS lesion involves C5′ chemistry on one strand and either C1′ or C4′ chemistry on the other; SS lesions are predominantly associated with the C5′ lesion (Goldberg & Kappen, 1994). C1027 differs in that C4′ chemistry on one strand is associated with either C5′ or C1′ chemistry on the complementary strand in the DS lesion; SS lesions are mainly due to the C4′ lesion (Figure 13). The different combination of chemistries involved in DS lesion generation for the two enediynes may be due to the fact that the distances between the two radical centers differ for the two antibiotics. C1027 involves a 1,4-benzene diradical, whereas neocarzinostatin utilizes a 2,6-indacene diradical.

It is also clear that the drug radical center involved in attack at A2 or A3 is more exposed to solvent than the radical involved in A1 attack. Thus, solvent methanol is highly effective in selectively quenching the former reaction and in preventing DS lesion formation. Further, the physical relationship of the drug radical center with the A2 and A3 attack sites provides for considerable flexibility in target selection by the abstracting radical. This is shown by experiments involving methanol containing carbon-bound deuterium, where a substantial isotope effect on the quenching reaction enables efficient protium abstraction from A2 or A3 and DS lesion formation. This flexibility in attack site selection is strikingly demonstrated in experiments where deuterium is substituted at C1′ of A2, resulting in almost total inhibition of attack at A2 and substantial shift of the reaction to hydrogen abstraction from C5′ of A3. Shuttling of the abstraction to a neighboring nucleotide has not been described before. Earlier experiments with neocarzinostatin chromophore have shown shuttling between two carbon attack sites (C5′ and C4′) of the same nucleotide depending on which sugar carbon possessed the deuterium.

The flexibility of the structure formed between drug and the DNA strand containing A2 and A3 is also demonstrated by the unexpected finding that within the one target sequence there are two attack sites, at A2 and A3, causing DS lesions with a common A1 site on the complementary strand. The affinity cleavage binding data are compatible with these lesions being due to a common drug-binding mode but one radical center having considerable leeway in target site selection. Strong additional support for a single mode of binding comes from the deuterium-induced shuttling of the attack to the adjacent nucleotide. It seems very unlikely that activated drug, bound in one mode, would be sufficiently stable in the radical form to be able to dissociate from the complex and rebind, still as the radical species, in the alternate binding mode.

The finding that the DS lesion involving A1 and A3 is staggered by two nucleotides in the 3′-direction is consistent with intercalation by the benzoxazine moiety of C1027 chromophore within the target sites on the complementary DNA strands, as has been demonstrated for neocarzinostatin chromophore (Goldberg, 1991; Gao et al., 1995a,b). This contrasts with the staggered three-nucleotide DS lesion generated by calicheamicin (Zein et al., 1988), which lacks an intercalating moiety. A DS lesion involving A1 and A2 which is staggered by only a single nucleotide in the 3′-direction is most unusual and best explained by the plasticity of the drug−DNA structure at the A2 and A3 sites. It seems very unlikely that this novel DS lesion, and the drug−DNA complex giving rise to it, would exist as an entirely independent lesion.

ACKNOWLEDGMENT

We thank Dr. Wei-tian Tan for providing 3′-phosphoglycolate-ended oligonucleotides as electrophoretic markers and Jeannie Thivierge for her excellent technical assistance.

REFERENCES

Chin, D. H., & Goldberg, I. H. (1993) *Biochemistry 32*, 3611−3616.

Cobuzzi, R. J., Jr., Kotsopoulos, S. K., Otani, T., & Beerman, T. A. (1995) *Biochemistry 34*, 583−592.

Dedon, P. C., & Goldberg, I. H. (1992) *Biochemistry 31*, 1909−1917.

Dedon, P. C., Salzberg, A. A., & Xu, J. (1993) *Biochemistry 32*, 3617−3622.

Durand, M., Chevrie, K., Chassignol, M., Thuong, N. T., & Maurizot, J. C. (1990) *Nucleic Acids Res. 18*, 6353−6359.

Gao, X., Stassinopoulos, A., Gu, J., & Goldberg, I. H. (1995a) *Bioorg. Med. Chem. 3*, 795−809.

Gao, X., Stassinopoulos, A., Rice, J. S., Goldberg, I. H. (1995b) *Biochemistry 34*, 40−49.

Giloni, L., Takeshita, M., Johnson, F., Iden, C., & Grollman, A. P. (1981) *J. Biol. Chem. 256*, 8608−8615.
Goldberg, I. H. (1991) *Acc. Chem. Res. 24*, 191−198.
Goldberg, I. H., & Kappen, L. S. (1994) in *Enediyne Antibiotics as Antitumor Agents* (Borders, D. B., & Doyle, T. W., Eds.) pp 327−362, Marcel Dekker, New York and Basel, Switzerland.
Han, H., & Dervan, P. B. (1993) *Proc. Natl. Acad. U.S.A. 90*, 3806−3810.
Hu, J. L., Xue, Y. C., Xie, M. Y., Zhang, R., Otani, T., Minami, Y., Yamada, Y., & Marunaka, T. (1988) *J. Antibiot. 41*, 1575−1579.
Iida, K., Ishii, T., Hirama, M., Otani, T., Minami, Y., & Yoshida, K. (1993) *Tetrahedron Lett. 34*, 4079−4082.
Kappen, L. S., & Goldberg, I. H. (1983) *Biochemistry 22*, 4872−4878.
Kappen, L. S., & Goldberg, I. H. (1989) *Biochemistry 28*, 1027−1032.
Kappen, L. S., & Goldberg, I. H. (1992a) *Biochemistry 31*, 9081−9089.
Kappen, L. S., & Goldberg, I. H. (1992b) *Proc. Natl. Acad. U.S.A. 89*, 6706−6710.
Kappen, L. S., Chen, C. Q., & Goldberg, I. H. (1988) *Biochemistry 27*, 4331−4340.
Kappen, L. S., Goldberg, I. H., Wu, S. H., Stubbe, J., Worth, L., Jr., & Kozarich, J. W. (1990) *J. Am. Chem. Soc. 112*, 2797−2798.
Kappen, L. S., Goldberg, I. H., Frank, B. L., Worth, L., Jr., Christner, D. F., Kozarich, W., & Stubbe, J. (1991) *Biochemistry 30*, 2034−2042.
Lee, M. D., Ellestad, G. A., & Borders, D. B. (1991) *Acc. Chem. Res. 24*, 235−243.
Leet, J., Schroeder, D. R., Langley, D. R., Colson, K. L., Huang, S., Klohr, S. E., Lee, M. S., Golik, J., Hofstead, S. J., Doyle, T. W., & Maston, J. A. (1993) *J. Am. Chem. Soc. 115*, 8432−8443.
Long, B. H., Olik, J., Forenza, S., Ward, B., Rehfuss, R., Dabrowiak, J. C., Catino, J. J., Musial, S. T., Brookshire, K. W., & Doyle, T. W. (1989) *Proc. Natl. Acad. Sci. U.S.A. 86*, 2−6.
McHugh, M. M., Woynarowski, J. M., Gawron, L. S., Otani, T., & Beerman, T. (1995) *Biochemistry 34*, 1805−1814.
Meschwitz, S. M., Schultz, R. G., Ashley, G. W., & Goldberg, I. H. (1992) *Biochemistry 31*, 9117−9121.
Minami, Y., Yoshida, K., Azum, R., Saeki, M., & Otani, T. (1993) *Tetrahedron Lett. 34*, 2633−2636.
Okuno, Y., Otsuka, M., & Sugiura, Y. (1994) *J. Med. Chem. 37*, 2266−2273.
Otani, T., Minami, Y., Marunaka, T., Zhang, R., & Xie, M. Y. (1988) *J. Antibiot. 41*, 1580−1585.
Otani, T., Yasuhara, T., Minami, Y., Shimazu, T., Zhang, R., & Xie, M. Y. (1991) *Agric. Biol. Chem. 55*, 407−417.
Robins, M. J., Wilson, J. S., & Hansske, F. (1983) *J. Am. Chem. Soc. 105*, 4059−4065.
Schroeder, D. R., Colson, K. L., Klohr, S. E., Zein, N., Langley, D. R., Mike, S. L., Matson, J. A., & Doyle, T. W. (1994) *J. Am. Chem. Soc. 116*, 9351−9352.
Stassinopoulos, A., & Goldberg, I. H. (1995) *Bioorg. Med. Chem. 3*, 713−721.
Stubbe, J., & Kozarich, J. W. (1987) *Chem. Rev. 87*, 1107−1136.
Sugiura, Y., & Matsumoto, T. (1993) *Biochemistry 32*, 5548−5553.
Sugiura, Y., Shiraki, T., Konishi, M., & Oki, T. (1990) *Proc. Natl. Acad. Sci. U.S.A. 87*, 3831−3835.
Vorbrüggen, H., & Bennua, B. (1981) *Chem. Ber. 114*, 1279−1286.
Worth, L., Jr., Frank, B. L., Christner, D. F., Absalon, M. J., Stubbe, J., & Kozarich, J. W. (1993) *Biochemistry 32*, 2601−2609.
Xu, Y. J., Li, D. D., & Zhen, Y. S. (1990) *Cancer Chemother. Pharmacol. 27*, 41−46.
Xu, Y. J., Li, D. D., & Zhen, Y. S. (1992) *Sci. Sin., Ser. B 8*, 814−819.
Xu, Y. J., Zhen, Y. S., & Goldberg, I. H. (1994) *Biochemistry 33*, 5947−5954.
Yang, C., Stassinopoulos, A., & Goldberg, I. H. (1995) *Biochemistry 34*, 2267−2275.
Zein, N., Sinha, A. M., McGahren, W. J., & Ellestad, G. A. (1988) *Science 240*, 1198−1201.
Zein, N., Colson, K. L., Leet, J. E., Schroeder, D. R., Solomon, W., Doyle, T. W., & Casazza, A. M. (1993) *Proc. Natl. Acad. Sci. U.S.A. 90*, 2822−2826.
Zhen, Y. S., Ming, X. Y., Yu, B., Otani, T., Saito, H., & Yamada, Y. (1989) *J. Antibiot. 42*, 1294−1298.
Zhen, Y. S., Xue, Y. C., & Shao, Y. G. (1994) *Kangshengsu 19*, 164−168.

BI951237O